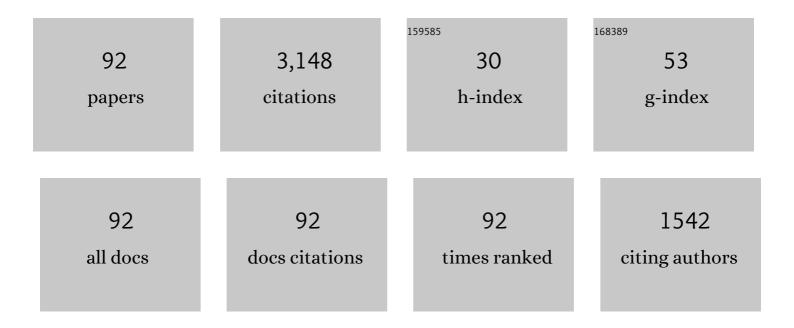
## Xiaolian Chao

List of Publications by Year in descending order

Source: https://exaly.com/author-pdf/8596976/publications.pdf Version: 2024-02-01



#	Article	IF	CITATIONS
1	High energy storage and colossal permittivity CdCu3Ti4O12 oxide ceramics. Ceramics International, 2022, 48, 4255-4260.	4.8	10
2	Bi0.5Na0.5TiO3-based ceramics with high energy storage density and good thermal stability. Journal of Materials Science: Materials in Electronics, 2022, 33, 2012-2019.	2.2	10
3	An Essential Role of Polymeric Adhesives in the Reinforcement of Acidified Paper Relics. Polymers, 2022, 14, 207.	4.5	4
4	Investigation of Deterioration for Large Outdoor Iron Statues Relics: A Case Research of Chairman MAO Iron Statue in Qinghai, China. Coatings, 2022, 12, 128.	2.6	1
5	Sodium bismuth titanate-based perovskite ceramics with high energy storage efficiency and discharge performance. Journal of Materiomics, 2022, 8, 1077-1085.	5.7	18
6	Enhanced energy storage properties and superior thermal stability in SNN-based tungsten bronze ceramics through substitution strategy. Journal of the European Ceramic Society, 2022, 42, 2781-2788.	5.7	21
7	Microscopic Imaging Technology Assisted Dynamic Monitoring and Restoration of Micron-Level Cracks in the Painted Layer of Terracotta Warriors and Horses of the Western Han Dynasty. Polymers, 2022, 14, 760.	4.5	1
8	Analytical Investigation of Jiatang Scroll Paintings in the Seventh Year of the Guangxu Era. Coatings, 2022, 12, 410.	2.6	2
9	High transparency and good electric properties in low symmetry BNT-based ceramics. Solid State Sciences, 2022, 129, 106906.	3.2	4
10	Excellent energy storage and discharge performances in Na <sub>1/2</sub> Bi <sub>1/2</sub> TiO <sub>3</sub> -based ergodic relaxors by enlarging the [AO <sub>12</sub> ] cages. Journal of Materials Chemistry C, 2022, 10, 8845-8853.	5.5	13
11	Significantly Enhanced Thermoelectric Performance Achieved in CuGaTe <sub>2</sub> through Dual-Element Permutations at Cation Sites. ACS Applied Materials & Interfaces, 2022, 14, 30046-30055.	8.0	8
12	High energy storage density realized in Bi0.5Na0.5TiO3-based relaxor ferroelectric ceramics at ultralow sintering temperature. Journal of the European Ceramic Society, 2021, 41, 368-375.	5.7	39
13	Ag+/W6+ co-doped TiO2 ceramic with colossal permittivity and low loss. Journal of Alloys and Compounds, 2021, 856, 157350.	5.5	33
14	A novel multifunctional ceramic with photoluminescence and outstanding energy storage properties. Chemical Engineering Journal, 2021, 408, 127368.	12.7	109
15	Coherent Sb/CuTe Core/Shell Nanostructure with Large Strain Contrast Boosting the Thermoelectric Performance of nâ€Type PbTe. Advanced Functional Materials, 2021, 31, 2007340.	14.9	30
16	Good dielectric performance and broadband dielectric polarization in Ag, Nb coâ€doped TiO <sub>2</sub> . Journal of the American Ceramic Society, 2021, 104, 2702-2710.	3.8	33
17	Application of Ethylene Oxide Gas and Argon Gas Mixture System Method for Scale Deacidification of Cellulose-Based Cultural Heritage Collections. Coatings, 2021, 11, 973.	2.6	2
18	High energy and power density achieved in Bi0.5Na0.5TiO3-based relaxor ferroelectric ceramics with excellent thermal stability. Journal of Alloys and Compounds, 2021, 875, 160005.	5.5	18

#	Article	IF	CITATIONS
19	Strained Endotaxial PbS Nanoprecipitates Boosting Ultrahigh Thermoelectric Quality Factor in nâ€Type PbTe Asâ€Cast Ingots. Small, 2021, 17, e2104496.	10.0	20
20	An Essential Role of Gelatin in the Formation Process of Curling in Long Historical Photos. Polymers, 2021, 13, 3894.	4.5	5
21	Synergy of Valence Band Modulation and Grain Boundary Engineering Leading to Improved Thermoelectric Performance in SnTe. ACS Applied Energy Materials, 2021, 4, 14608-14617.	5.1	15
22	Grain boundary engineering that induces ultrahigh permittivity and decreased dielectric loss in CdCu <sub>3</sub> Ti <sub>4</sub> O <sub>12</sub> ceramics. Journal of the American Ceramic Society, 2020, 103, 1230-1240.	3.8	39
23	Controllable synthesis of (Ba0.85Ca0.15)(Zr0.1Ti0.9)O3 submicron sphere by hydroxide co-precipitation method. Ceramics International, 2020, 46, 28285-28291.	4.8	7
24	One-Step Reinforcement and Deacidification of Paper Documents: Application of Lewis Base—Chitosan Nanoparticle Coatings and Analytical Characterization. Coatings, 2020, 10, 1226.	2.6	14
25	Regulation of energy density and efficiency in transparent ceramics by grain refinement. Chemical Engineering Journal, 2020, 390, 124566.	12.7	140
26	Grain engineering inducing high energy storage in CdCu3Ti4O12 ceramics. Ceramics International, 2020, 46, 14425-14430.	4.8	37
27	Ultrahigh storage density achieved with (1-x)KNN-xBZN ceramics. Journal of the European Ceramic Society, 2020, 40, 2936-2944.	5.7	57
28	Superior comprehensive energy storage properties in Bi0.5Na0.5TiO3-based relaxor ferroelectric ceramics. Chemical Engineering Journal, 2020, 388, 124158.	12.7	279
29	A compromise between piezoelectricity and transparency in KNN-based ceramics: The dual functions of Li2O addition. Journal of the European Ceramic Society, 2020, 40, 2331-2337.	5.7	38
30	Good thermal stability, giant permittivity, and low dielectric loss for X9Râ€ŧype (Ag <sub>1/4</sub> Nb <sub>3/4</sub> ) <sub>0.005</sub> Ti <sub>0.995</sub> O <sub>2</sub> ceramics. Journal of the American Ceramic Society, 2019, 102, 970-975.	3.8	27
31	Bi <sub>0.5</sub> Na <sub>0.5</sub> TiO <sub>3</sub> -based relaxor ferroelectric ceramic with large energy density and high efficiency under a moderate electric field. Journal of Materials Chemistry C, 2019, 7, 10514-10520.	5.5	155
32	Enhanced energy density and thermal stability in relaxor ferroelectric Bi0.5Na0.5TiO3-Sr0.7Bi0.2TiO3 ceramics. Journal of the European Ceramic Society, 2019, 39, 4778-4784.	5.7	182
33	High-efficiency synthesis of high-performance K0.5Na0.5NbO3 ceramics. Powder Technology, 2019, 346, 248-255.	4.2	23
34	Evaluation of birefringence contribution to transparency in (1-x)KNN-xSr(Al0.5Ta0.5)O3 ceramics: A phase structure tailoring. Journal of Alloys and Compounds, 2019, 798, 669-677.	5.5	19
35	Excellent optical transparency of potassium-sodium niobate-based lead-free relaxor ceramics induced by fine grains. Journal of the European Ceramic Society, 2019, 39, 3684-3692.	5.7	27
36	Step-Up Thermoelectric Performance Realized in Bi <sub>2</sub> Te <sub>3</sub> Alloyed GeTe via Carrier Concentration and Microstructure Modulations. ACS Applied Energy Materials, 2019, 2, 1616-1622.	5.1	25

#	Article	IF	CITATIONS
37	Simultaneous realization of broad temperature stability range and outstanding dielectric performance in (Ag+, Ta5+) co–doped TiO2 ceramics. Journal of Alloys and Compounds, 2019, 783, 423-427.	5.5	28
38	Relaxor behaviors and electric response in transparent 0.95(K0.5Na0.5NbO3)-0.05Ca(Zr ZnyNbz)1.025O3 ceramics with low-symmetric structure. Ceramics International, 2019, 45, 3961-3968.	4.8	19
39	Submicron barium calcium zirconium titanate ceramic for energy storage synthesised via the co-precipitation method. Materials Research Bulletin, 2019, 111, 259-266.	5.2	32
40	Simultaneous realization of high transparency and piezoelectricity in low symmetry <scp>KNN</scp> â€based ceramics. Journal of the American Ceramic Society, 2019, 102, 3498-3509.	3.8	27
41	Effects of preparation method on the microstructure and electrical properties of tungsten bronze structure Sr2NaNb5O15 ceramics. Ceramics International, 2019, 45, 558-565.	4.8	12
42	Leadâ€free (K,Na)NbO <sub>3</sub> â€based ceramics with high optical transparency and large energy storage ability. Journal of the American Ceramic Society, 2018, 101, 2321-2329.	3.8	130
43	Origin of giant permittivity in Ta, Al co-doped TiO2: Surface layer and internal barrier capacitance layer effects. Ceramics International, 2018, 44, 5768-5773.	4.8	36
44	Improved transmittance and ferroelectric properties realized in KNN ceramics via SAN modification. Journal of the American Ceramic Society, 2018, 101, 5127-5137.	3.8	39
45	Fabrication and characterization of CdCu3Ti4O12 ceramics with colossal permittivity and low dielectric loss. Materials Letters, 2018, 210, 301-304.	2.6	33
46	Influence of Bi nonstoichiometry on the energy storage properties of 0.93KNN–0.07Bi <sub><i>x</i></sub> MN relaxor ferroelectrics. Journal of Advanced Dielectrics, 2018, 08, 1830006.	2.4	28
47	Excellent near-infrared transparency realized in low-symmetry orthorhombic (K,Na)NbO3-based submicron ceramics. Scripta Materialia, 2018, 154, 64-67.	5.2	15
48	Effect of Zr doping on dielectric properties and grain boundary response of CdCu3Ti4O12 ceramics. Ceramics International, 2018, 44, 20311-20321.	4.8	21
49	Effect of Carbon Nanotubes on the Structure, Internal Loss Storage, and Damping–Absorption Properties of CNT/PZT/RTV. Polymer-Plastics Technology and Engineering, 2017, 56, 1196-1202.	1.9	1
50	Dielectric Properties of Tungsten Copper Barium Ceramic as Promising Colossal-Permittivity Material. Journal of Electronic Materials, 2017, 46, 4697-4700.	2.2	1
51	Structure and Electrical Properties of Sr1.85Ca0.15NaNb5O15 Ceramics with Addition of Multivalence Oxides (MnO2, PbO2). Journal of Electronic Materials, 2017, 46, 5967-5977.	2.2	2
52	Enhanced transmittance and piezoelectricity of transparent K <sub>0.5</sub> Na <sub>0.5</sub> NbO <sub>3</sub> ceramics with Ca(Zn <sub>1/3</sub> Nb <sub>2/3</sub> )O <sub>3</sub> additives. RSC Advances, 2017, 7, 28428-28437.	3.6	53
53	Structure, electrical properties and reaction mechanism of (Ba0.85Ca0.15)(Zr0.1Ti0.9)O3 ceramics synthesized by the molten salt method. Ceramics International, 2017, 43, 11920-11928.	4.8	10
54	Electrical and transparent properties induced by structural modulation in (Sr0.925Ca0.075)2.5–0.5Na Nb5O15 ceramics. Journal of the European Ceramic Society, 2017, 37, 2605-2613.	5.7	17

#	Article	IF	CITATIONS
55	Fabrication and enhanced characterization of copper powder filled copper calcium titanate/poly(vinylidene difluoride) composite. Journal of Materials Science: Materials in Electronics, 2017, 28, 5435-5439.	2.2	3
56	Excellent Transmittance Induced Phase Transition and Grain Size Modulation in Leadâ€Free (1– <i>x</i> )(K <sub>0.5</sub> Na <sub>0.5</sub> )NbO <sub>3</sub> – <i>x</i> LaBiO <sub>3</sub> Ceramics. Journal of the American Ceramic Society, 2016, 99, 2055-2062.	3.8	39
57	Structure, dielectric property and impedance spectroscopy of La2/3Cu3Ti4O12 ceramics by sol–gel method. Journal of Materials Science: Materials in Electronics, 2016, 27, 8980-8990.	2.2	10
58	Improved dielectric properties and grain boundary response in neodymium-doped Y2/3Cu3Ti4O12 ceramics. Journal of Alloys and Compounds, 2016, 678, 273-283.	5.5	28
59	Low temperature sintering and dielectric properties of (Ba0.85Ca0.15)(Ti0.9Zr0.1)O3â^'xCu2+ ceramics obtained by the sol-gel technique. Ceramics International, 2016, 42, 18037-18044.	4.8	12
60	Transparency of K0.5N0.5NbO3–Sr(Mg1/3Nb2/3)O3 lead-free ceramics modulated by relaxor behavior and grain size. Ceramics International, 2016, 42, 17963-17971.	4.8	57
61	Dielectric responses of Na0.65Bi0.45Cu3Ti4O12 ceramics based on the composition design of changing the Na/Bi ratio. Journal of Materials Science: Materials in Electronics, 2016, 27, 2221-2227.	2.2	1
62	Electrical Characterization Induced by Structural Modulation inâ£(Ca0.28Ba0.72)2.5–0.5x (Na0.5K0.5) x Nb5O15 Ceramics. Journal of Electronic Materials, 2016, 45, 104-115.	2.2	5
63	Aging behavior and electrical properties of low-temperature sintered (Ba, Ca)(Ti, Zr)O 3 -Ba(Cu, W)O 3 ceramics and plate loudspeaker. Sensors and Actuators A: Physical, 2016, 237, 9-19.	4.1	9
64	Synthesis, structure, dielectric, piezoelectric, and energy storage performance of (Ba0.85Ca0.15)(Ti0.9Zr0.1)O3 ceramics prepared by different methods. Journal of Materials Science: Materials in Electronics, 2016, 27, 5047-5058.	2.2	59
65	The enhancing performance of (Ba0.85Ca0.15Ti0.90Zr0.10)O3 ceramics by tuning anatase–rutile phase structure. Materials Research Bulletin, 2016, 76, 450-453.	5.2	11
66	Diffusion phase transition and impedance spectroscopy of Bi2O3/CuO co-doped BCZT lead-free ceramics. Journal of Materials Science: Materials in Electronics, 2016, 27, 3217-3226.	2.2	11
67	Tailoring Electrical Properties and the Structure Evolution of (Ba0.85Ca0.15)(Ti0.90Zr0.10)1â^'x Li4x O3 Ceramics with Low Sintering Temperature. Journal of Electronic Materials, 2016, 45, 802-811.	2.2	12
68	Optical and electrical properties of pressureless sintered transparent (K0.37Na0.63)NbO3-based ceramics. Ceramics International, 2016, 42, 4648-4657.	4.8	32
69	Phase transition and improved electrical performance of Ba0.85Ca0.15Zr0.1Ti0.9O3–Ca0.28Ba0.72Nb2O6 ceramics with high Curie temperature. Materials and Design, 2016, 89, 465-469.	7.0	32
70	Phase evolution and enhanced electrical properties of (Ba0.85Ca0.15â^'x Y x )(Zr0.1Ti0.9)O3 lead-free ceramics. Journal of Materials Science: Materials in Electronics, 2015, 26, 5217-5225.	2.2	19
71	Role of structural modulation in electrical properties of tungsten bronze (Ca0.28Ba0.72)2.5â^'0.5Na Nb5O15 ceramics. Journal of Alloys and Compounds, 2015, 632, 368-375.	5.5	29
72	Dielectric Properties and Impedance Spectroscopy of MnCO <sub>3</sub> â€Modified (Ba <sub>0.85</sub> Ca <sub>0.15</sub> )(Zr <sub>0.1</sub> Ti <sub>0.9</sub> )O <sub>3</sub> Leadâ€Free Ceramics. Journal of the American Ceramic Society, 2015, 98, 1506-1514.	3.8	72

#	Article	IF	CITATIONS
73	Ba(Cu0.5W0.5)O3-induced sinterability, electrical and mechanical properties of (Ba0.85Ca0.15Ti0.90Zr0.10)O3 ceramics sintered at low temperature. Materials Research Bulletin, 2015, 66, 16-25.	5.2	22
74	Synthesis, dielectric properties of Bi2/3Cu3Ti4O12 ceramics by the sol–gel method. Journal of Materials Science: Materials in Electronics, 2015, 26, 1959-1968.	2.2	16
75	Phase Formation and Enhanced Dielectric Response of Y <sub>2/3</sub> Cu <sub>3</sub> Ti <sub>4</sub> O <sub>12</sub> Ceramics Derived from the Sol–Gel Process. Journal of the American Ceramic Society, 2015, 98, 795-803.	3.8	40
76	Effect of CaCu3Ti4O12 powders prepared by the different synthetic methods on dielectric properties of CaCu3Ti4O12/polyvinylidene fluoride composites. Journal of Materials Science: Materials in Electronics, 2015, 26, 3044-3051.	2.2	22
77	Electrical properties and low temperature sintering of BiAlO3 doped (Ba0.85Ca0.15)(Zr0.1Ti0.9)O3 lead-free piezoelectric ceramics. Journal of Materials Science: Materials in Electronics, 2015, 26, 7331-7340.	2.2	18
78	Effects of ZnO Content on Piezoelectric, Dielectric, and Magnetic Properties of Sr-Modified PZT–PMW–PNN/(Ni-Co-Cu) ME Composites. Journal of Electronic Materials, 2015, 44, 3415-3421.	2.2	1
79	Microstructure, electrical properties, strain and temperature stability of (K, Na, Li)(Nb, Ta)O3 ceramics: The effect of BiFeO3 additive. Ceramics International, 2015, 41, 12887-12895.	4.8	13
80	Differentiated Electric Behaviors of <scp><scp>La</scp></scp> <sub>2/3</sub> <scp><scp>Cu</scp><sub>3</sub><scp><scp>Ti</scp>Ceramics Prepared by Different Methods. Journal of the American Ceramic Society, 2014, 97, 2154-2163.</scp></scp>	)> <b>≋sa</b> ub>4∢	:/sub> <scp></scp>
81	Study on low temperature sintering and electrical properties of CuO-doped Ca0.28Ba0.72Nb2O6 ceramics. Journal of Materials Science: Materials in Electronics, 2014, 25, 1605-1611.	2.2	0
82	Polymorphic structure evolution and large piezoelectric response of lead-free (Ba,Ca)(Zr,Ti)O3 ceramics. Applied Physics Letters, 2014, 104, .	3.3	80
83	Phase Transition Behavior and Large Piezoelectricity Near the Morphotropic Phase Boundary of Leadâ€Free ( <scp><scp>Ba</scp></scp> <sub>0.85</sub> <scp><scp>Ca</scp></scp> <sub>0.15</sub> )( <scp><scp>ZrCeramics, Journal of the American Ceramic Society, 2013, 96, 496-502.</scp></scp>	p>	:sub≻0.1
84	Phase transition behavior and electrical properties of lead-free (Ba1â^'xCax)(Zr0.1Ti0.9)O3 piezoelectric ceramics. Journal of Applied Physics, 2013, 113, .	2.5	99
85	The Lowered Dielectric Loss and Grainâ€Boundary Effects in <scp><scp>La</scp></scp> â€doped <scp><scp>Y</scp></scp> <sub>2/3</sub> <scp>Cu</scp> 3 <scp>Ti</scp> Ceramics. Journal of the American Ceramic Society, 2013, 96, 3883-3890.	>< <b>sub</b> >4 </td <td>ˈsuadə&gt; &lt; scp &gt; &lt;</td>	ˈsuadə> < scp > <
86	Performance of Room Temperature Vulcanized (RTV) Silicone Rubber-Based Composites: DBDPO/RTV and DBDPE/Sb <sub>2</sub> O <sub>3</sub> /RTV. Polymer-Plastics Technology and Engineering, 2012, 51, 1245-1250.	1.9	14
87	Phase structures, electrical properties and temperature stability of (1â^'x)[(K0.458Na0.542)0.96Li0.04](Nb0.85Ta0.15)O3–xBiFeO3 ceramics. Journal of Alloys and Compounds, 2012, 518, 1-5.	5.5	29
88	Giant Dielectric Constant and Good Temperature Stability in <scp><scp>Y</scp></scp> <sub>2/3</sub> <scp>Cu</scp> <sub>3</sub> <scp><scp>Ti</scp> Ceramics. Journal of the American Ceramic Society, 2012, 95, 2218-2225.</scp>	>< <b>318</b> b>4 </td <td>suba<scp>&lt;</scp></td>	suba <scp>&lt;</scp>
89	Fabrication, temperature stability and characteristics of Pb(Zr Ti) Tj ETQq1 1 0.784314 rgBT /Overlock 10 Tf 50 1 38, 3377-3382.	07 Td ()O3 4.8	3–Pb(Zn1/ 17
90	Effect of Sintering Process on Characteristics of Multilayer Piezoelectric Pb(Mg1/3Nb2/3)O3–Pb(Zn1/3Nb2/3)O3–Pb(Zr,Ti)O3Ceramic Transformers. Japanese Journal of Applied Physics, 2007, 46, 6746-6750.	1.5	9

#	Article	IF	CITATIONS
91	Structure, electrical properties and energy storage performance of BNKT-BMN ceramics. Journal of Materials Science: Materials in Electronics, 0, , 1.	2.2	5
92	A new family of high temperature stability and ultra-fast charge–discharge KNN-based lead-free ceramics. Journal of Materials Science, 0, , 1.	3.7	6